Design, Simulation, and Prototype of an 18-Wheeler Electric Vehicle with Range Extension using Solar PV and Regenerative Braking

IAN LIM, JARED FAUNI, ETHAN CHEN, LESLY MOUNGANG MBEUMO, CLARISSA SIMENTAL, JONATHAN VAN ZUYLEN, ARTURO TIERRABLANCA, HA THU LE*
Department of Electrical and Computer Engineering,
California State Polytechnic University, Pomona,
Pomona, California 91768,
UNITED STATES OF AMERICA

**Corresponding Author*

Abstract: – In response to California's initiative to propel the advancement of hybrid and electric vehicles toward achieving zero emissions, this study undertakes the design of a hybrid 18-wheeler aligning with the state's stringent standards. The motivation stems from the imperative need to address the research and development in the domain of hybrid/electric class 8 vehicles, specifically focusing on the pivotal segment of 18-wheelers. The research team developed a realistic theoretical design, verified it using MATLAB Simulink simulation, and ultimately built a prototype. The truck's novel features, namely, 60% electric power, regenerative braking, and solar PV for range extension, are included in the design and partially implemented in the prototype. Two motors, a DC and an AC, are used as the prototype drives where the system control is mostly automatic. Simulation of the electric 18-wheeler design shows that the model works properly. It follows the speed command closely while the acceleration and deceleration behaviors are normal. Testing of the prototype shows that it functions appropriately. The DC motor speed can be regulated over a wide speed range while the AC motor can run at two different speeds as designed. The prototype microcontroller logic is followed, ensuring safe operation of the solar PV system and the battery, and effective control of the motors. Overall, the project succeeded in achieving a harmonious blend of simulation, design, and physical implementation. It can be used as an engineering and public education tool. Further, by exploring cutting-edge technologies such as regenerative braking and solar power for truck range extension, the project contributes to raising vehicle efficiency and finding sustainable transportation solutions, which make the transportation sector more friendly to the environment.

Key-Words: - Class 8 vehicle, electric vehicle, 18-wheeler, hybrid vehicle, prototype, regenerative braking, solar PV, truck, zero-emission vehicle.

Received: November 20, 2023. Revised: December 10, 2023. Accepted: December 17, 2023. Published: December 31, 2023.

1 Introduction

Electric vehicles (EVs) offer multiple benefits compared to their diesel engine counterparts. According to the EPA, transportation is responsible for almost 30% of U.S. greenhouse gas emissions, [1]. A modern diesel-powered truck releases, on average, 223 tons of CO2 into the atmosphere every year, [2]. The improvement of fuel efficiency of semi-trucks has become stagnant. The average fuel efficiency of modern trucks is only 6.5MPG. This is less than 1 MPG better compared to fuel efficiency in 1973, [3].

Most of the environmental impact that is created by EVs comes from the manufacturing process. This issue has been improving in recent years by lowering the carbon footprint of battery production, [4]. Transportation companies can also benefit from the long-term ownership of EVs. The estimated annual maintenance is 18% to 45% cheaper than diesel semis and they are often much simpler, [3]. Further, EVs are friendly to the environment and efficient in terms of energy usage so transition to EVs can be a cost-effective approach, [5]. Though, there are obstacles to EV adoption, namely, insufficient range, high cost, and inadequate charging infrastructure, [6]. Another challenge that impedes EV usage is their high power demand, which can create stresses for their host power distribution systems, especially in residential areas where the feeder circuits are weak, [7].

To solve the EV-related problems, multiple technologies have been developed to increase the range and efficiency of electric vehicles, as well as expand the EV charging infrastructure. One technology is to use solar PV to charge the car battery, either when driving or being parked in the sun. This technology can potentially increase the vehicle range, reduce their dependence on charging networks, and lower power demand on the power grid.

Regenerative braking is another technology that can help solve EV-related problems, [8], [9]. It captures some kinetic energy from the car wheels that would otherwise be lost during braking periods to run the car's electric machine as a generator to produce energy. This energy is stored in the battery for later use which enhances the vehicle's range and efficiency.

The stress caused by EV high-power demand on the power grid can be alleviated by building big solar-powered charging stations at truck stops or shipping centers. Station and charger can be regulated by a charging management system where vehicles are prioritized based on their battery level. Investigations have also been made into larger 3-level systems that regulate different clusters of chargers as well as individual vehicles into different voltage level groups to minimize impact on the distribution grid, [10].

Innovative solutions such as smart bi-directional chargers and making use of propulsion systems for charging may also help with grid strain in the coming years, [11]. In addition, the government plans to expand the grid through the Grid Resilience and Innovation Partnerships program and has made available over $3.9 billion towards this goal, [12].

Last but not least, alternative battery materials are being investigated for EVs, which can replace lithium ions to some extent. While lithium-ion batteries are currently the most widely used, they have limitations in terms of their energy density, safety, and environmental impact, [13]. Lithium-ion batteries are fairly expensive and only have a shelf life of about 15 years before needing to be replaced, [14]. The search for alternative materials has the potential to improve the performance and sustainability of electric vehicles and expand their popularity even further, [15].

A project that investigates, simulates, and constructs a practical model of an electric vehicle with built-in solar charging, regenerative braking, and an alternative battery material has the potential to further benefit the current technology found in electric vehicles, [16]. Given the need to address fuel efficiency and carbon emission requirements of large trucks, we aim to design an 18-wheeler, where its range is extended by solar PV and regenerative braking. By exploring the potential of these technologies, our project can contribute to the development of more efficient, sustainable, and accessible transportation options. The truck design, its simulation, and prototyping are described in the following sections.

2 Truck Engine and Drivetrain Design and Simulation

While hybrid and fully electric options have been growing in popularity in recent years due to new laws and regulations, the current technology is nowhere near the ambitious standards that places like California have set in place, [17]. At the heart of the vehicle is the power train. More specifically, the engine configuration is the key to achieving these lofty goals. One of the first features one needs to determine for a hybrid configuration is the ratio between the electric motor and combustion engine, [18].

For this project, we aim to comply with the California standards and guidelines. California has only established rough guidelines and target years for certain percentage sales of zero-emission vehicles that progressively get stricter. Under the current Advanced Clean Trucks (ACT) rule, enacted by the California Air Resources Board (CARB) in June 2020, 5-9% of class 4-8 trucks sold in the state must be ZEVs (zero emission vehicles) by 2024. The CARB hopes to increase the ZEV percentage to 30% by 2030, [19].

These percentages also pertain to hybrid vehicles, essentially increasing the electric ratio of the powertrain alongside the outright sales of pure ZEVs. For class 2 vehicles, such as passenger cars, hybrids are much more efficient than conventional vehicles, achieving anywhere from 10 to 15% increased energy efficiency, [20]. For a class 8 standard 18-wheeler, it is much more difficult to design and optimize a hybrid/electric setup given the additional load induced from the cargo of the semi-trailer, [21]. While class 2 cars can achieve a decent electric mileage ratio, there is a significant drop for 18 wheelers.

With the limited offerings on the market at present, a typical hybrid 18-wheeler could only achieve 5-7% of electric range. An industry leader, all-electric Tesla Semi Truck, has its bevy of issues. Given the 1000-mile-plus range of a standard diesel semi, which would require a very long charging time if battery is solely used; hybrid options for

large trucks are needed to comply with new standards and regulations, [22].

2.1 Drivetrain Configuration

Following the regulations, we seek to design an engine that is 60% electric and 40% combustion engine. To do this, we need to drastically increase the design capabilities, such as battery capacity and electric motor power, to ensure the required torque and horsepower for the huge truck.

The first step to implementing our project was to create a base vehicle design on which to implement our design. There are 3 types of drivetrains for hybrid vehicles. The drivetrain design determines how the electric motor works in conjunction with the diesel engine, [23]. This drivetrain affects the vehicle efficiency and fuel consumption. The types are Series, Parallel, and Series Parallel, [24]. We decided to start with the Series design because it is the simplest hybrid configuration, which will simplify our intended computer-based simulation. In a series hybrid, the electric motor is the only means of providing power to the wheels. The Diesel engine provides partial power to the Electric motor and a large battery bank provides the remaining power that it needs. Figure 1 illustrates this design.

As said, the series configuration was chosen as our initial design for the drivetrain, as it was the simplest hybrid configuration. Choosing between a series and parallel configuration for a hybrid vehicle involves trade-offs that impact performance, efficiency, and complexity. Series configurations, characterized by an electric motor as the sole power source to the wheels, are more efficient than internal combustion engines in traffic conditions where the vehicles have frequent stops and restarts. A series configuration can switch between battery and engine power, conserving the engine for more efficient situations. However, the series configuration requires a larger battery and electric motor, along with a generator, making them more costly compared to parallel drivetrains.

In contrast, parallel configurations use both the engine and electric motor collaboratively, eliminating the inefficiencies of power conversion seen in series hybrids. This makes a parallel configuration more efficient on highways, but there is less efficiency in stop-and-go traffic conditions. Parallel hybrid design would require a smaller battery, relying on regenerative braking and the motor acting as a generator for recharging. We selected a Parallel hybrid drivetrain (Figure 2) for our truck design and simulation.

2.2 Specifications

Our Parallel hybrid design is based on a 40% diesel and 60% Electric Hybrid ratio. The following assumptions were made based on current semi-truck standards to calculate the motor size, battery size, and other specifications, [25]:

- Total Horsepower ≥ 500hp ≈ 373kW
- Average RPM = 1500 rpm
- Efficiency of the Electric motor = 75%
- 5-hour battery power

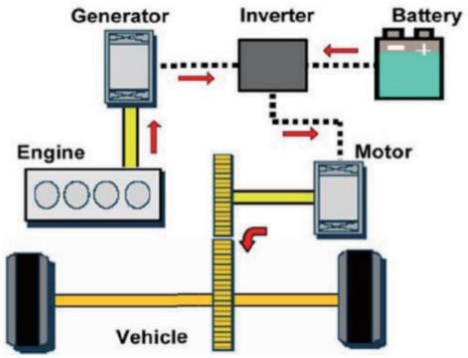

Fig. 1: Series hybrid drivetrain configuration, [26]

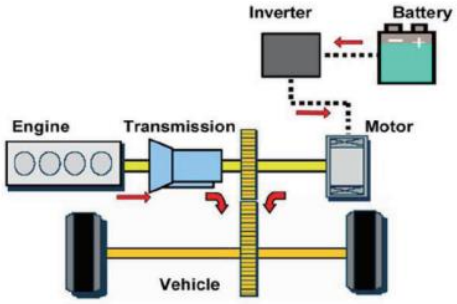

Fig. 2: Parallel hybrid drivetrain configuration, [26]

The truck's required torque must be at least 373kW or 500hp so the final power is designed to be 400kW, [27]. The diesel engine and the battery must be able to supply 40% and 60% of the truck's total power demand, respectively. Therefore, the diesel engine supplies a torque equivalent to 160kW, and the battery capacity needed to power the electric motor is 240kWh for 1 hour or 1200kWh for 5 hours.

2.3 Simulation of truck design

To explore the behavior of our truck design, we simulate it using MATLAB Simulink. The blocks used to represent the truck components are taken from the Simscape library. Figure 3 shows the basic architecture of a parallel hybrid transmission system, [28], which is implemented in Simulink for simulation. Figure 4, Figure 5 and Figure 6 shows

some simulation results. Individual components and parameters are provided in Figures A1, A2, A3, A4, A5, A6, A7, A8, A9 and A10 in Appendix.

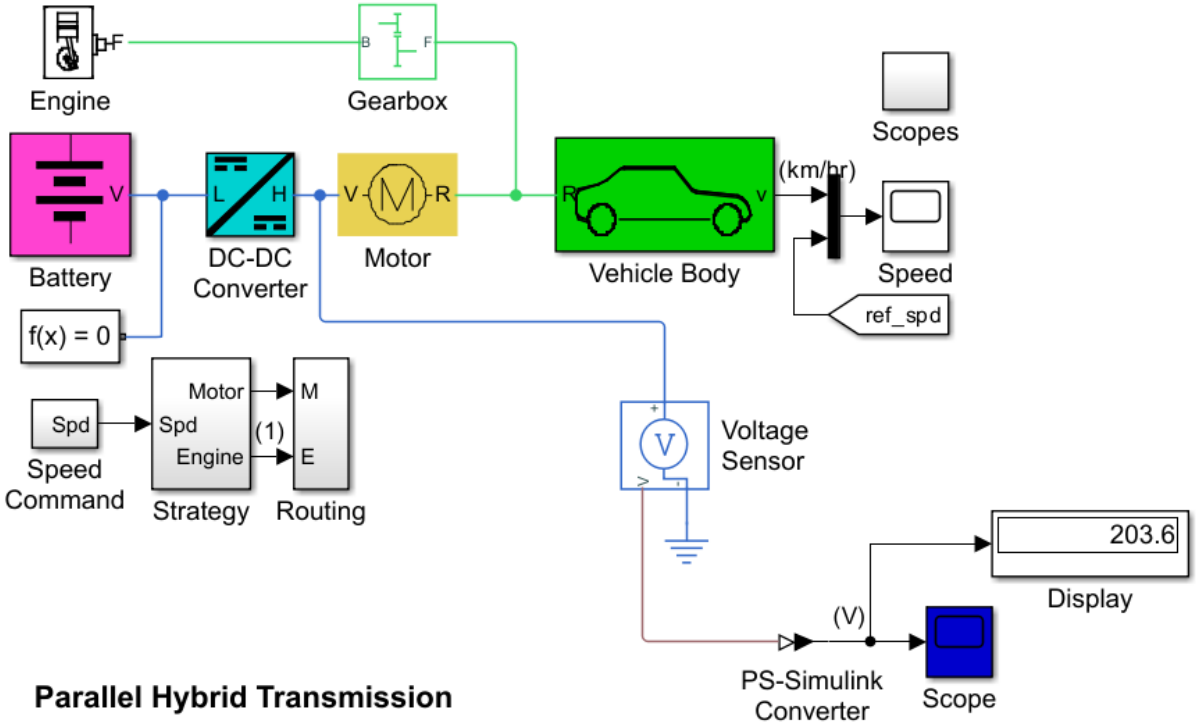

Fig. 3: MATLAB Simulink based truck model for simulation
(Individual components and parameters are provided in Appendix)

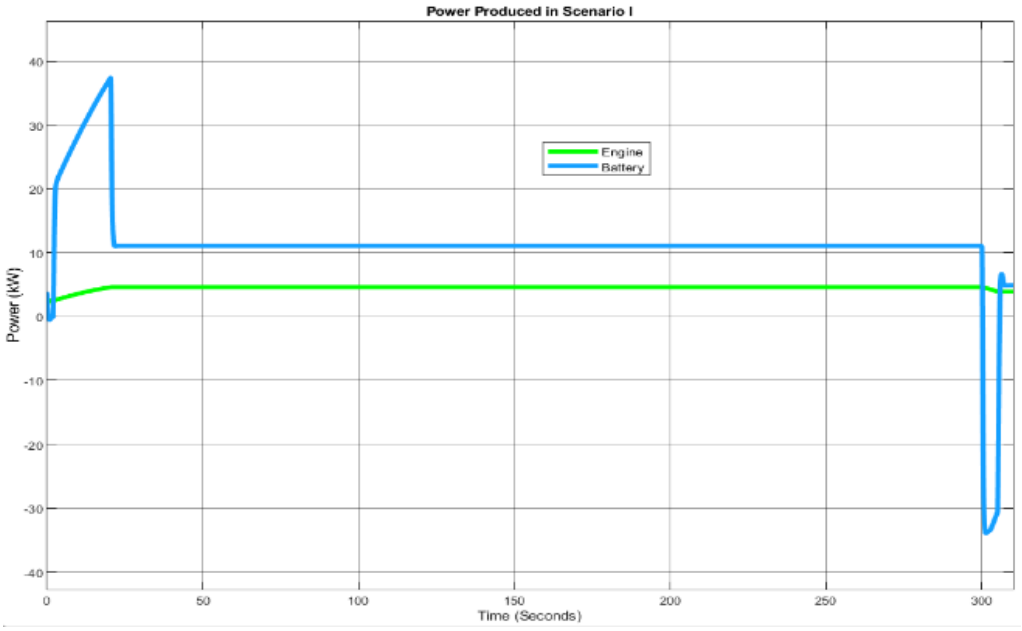

Fig. 4: Power output of battery and combustion engine in Scenario 1
(The truck model follows the speed command in Figure 7. The battery provides more power during the vehicle acceleration (around 22s) while the combustion engine is used to deliver the power required to maintain the desired speed. The power output of the battery and the engine is flat when the vehicle speed is constant)

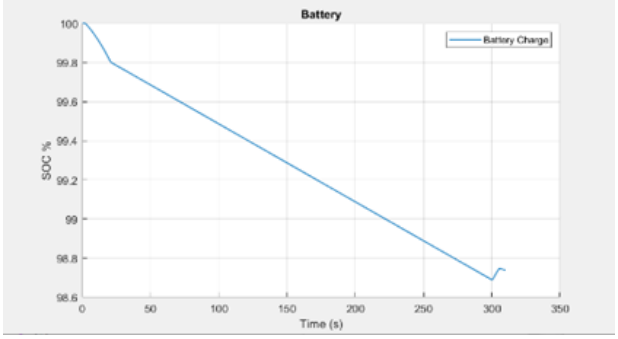

Fig. 5: State of charge of the battery

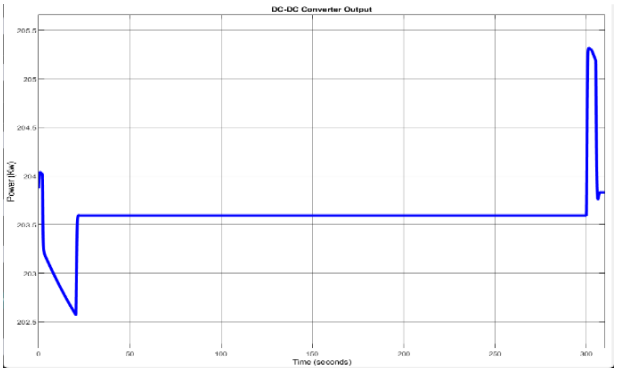

Fig. 6: Output of the DC-DC converter

2.3.1 Electrical System Parameters and Setting

Simulation setting: The simulation works by applying electrical power from the battery in parallel with the combustion engine, i.e., the battery drives the electric motor. The motor then applies electrical torque at the wheel axle, but it could also be applied to the engine flywheel. In this simulation, the vehicle accelerates, maintains the desired speed, and then decelerates back to zero or a predetermined speed. The power management control uses only electrical power to affect the maneuver while the combustion engine is only used to deliver the power required to maintain the desired speed.

Motor and Drive block: Parameters for this block are shown in Figure A10 in the Appendix. The maximum power of the electric motor is 240kW and the speed is 1500rpm. The Motor and Drive block incorporate initial losses through a first-order model, factoring in overall efficiency tied to a specified speed and torque input.

The parameters (motor and drive overall efficiency, speed for efficiency measurement, and torque for efficiency measurement) determine the efficiency characteristics. Utilizing this speed and torque data, the block constructs a torque-speed envelope that caps the input torque. This capped value dictates the torque the motor interacts with, termed $\tau elec$, and guides the computation of electrical losses within the system.

Battery block: The battery state of charge (SOC) can be seen in Figure 5. The power of the block is calculated using the basic power formula in [29]. During the simulation, the maximum power output of the battery is 37 kW which occurs at the point where the vehicle switches from acceleration to deceleration at time t= 20 sec. The power usage remains constant from the time the vehicle is idle.

A calculation block (not shown in Figure 3) takes the signal produced from the voltage sensor and current sensor to calculate the power usage, charge, and power loss of the battery.

Battery capacity refers to the overall quantity of electrical charge produced through electrochemical reactions within the battery and is typically denoted in terms of its capacity measured in ampere-hours (Ah). The capacity rating indicates how much charge the battery can hold and deliver over a certain period, [30].

The SOC represents the amount of remaining power in a battery relative to its total rated power that can be discharged under specific conditions and at a specified rate. The effect of the environment is not considered in the discharge capacity of the battery. The charge/discharge efficiency of a battery provides limited insight into actual efficiency, [31].

Ideal Transformer and DC-DC Converter: The ideal transformer block models an ideal power-conserving transformer that can represent a solid-state DC-DC converter, [32]. Utilizing a transformer becomes advantageous when a substantial step-up or step-down conversion ratio is needed. The careful selection of the transformer turns ratio enables more efficient optimization of the converter. By precisely choosing this ratio, it becomes possible to minimize the voltage or current pressures experienced by the transistors and diodes within the system. This minimization of stress leads to enhanced efficiency and decreased costs in the overall setup. The DC-DC converter is used to step down the battery voltage from 515 V to 203.8 V. From the output in Figure 6, we can see that the DC-DC converter works properly with zero ripples.

Strategy block: It converts the vehicle speed from kilometers per hour to rotations per minute. The engine throttle demand is calibrated to ensure that, during startup, the combustion engine supplies the minimum necessary power to maintain the vehicle's constant speed. Consequently, at this point, the battery power remains nearly depleted. Simultaneously, the motor RPM demand is synchronized to mirror the speed requested for the vehicle.

2.3.2 Mechanical System Parameters and Setting

Engine block: The diesel engine is represented using Simscape "Generic Engine" block (Annotated as "Engine" in Figure 3). This "Generic Engine" represents an internal combustion engine of either spark-ignition or diesel type. The engine parameters for simulation are shown in Figure A7 of the Appendix. We utilize a throttle signal to drive the engine. A throttle signal suits our needs better given its simplicity. It represents driver input which is more intuitive considering a driver trying to reach a certain output power level. It is also much easier to tune but can offer less direct control of the system given that it is reliant on the engine's response to throttle input.

The engine block calculates power demand based on this throttle in conjunction with engine speed. Since we can set different engine types, spark ignition, and diesel have their unique coefficients to use as the model is predicated on a third-order polynomial. The coefficients utilized define peak power and torque.

Vehicle Body block: For our parallel configuration, we attach the engine to the tangible vehicle body (Green "Vehicle Body" block in Figure 3) via a gearbox (transmission). This enables us to manage torque, and speed, and provide additional functionality such as reverse operation of the vehicle.

As far as mechanical factors are concerned, the gearbox block enforces a fixed rotation ratio between the base gear (B) and the follower gear (F). This ratio can be altered based on whether one wants them to follow the same direction for rotation. For this project, we have them rotate in the same direction.

The Vehicle Body block encompasses the tires and the truck's physical body. According to the California Department of Transportation, the maximum allowed weight of a class 8-18-wheeler is 80,000 pounds (approximately 36,287 kg), [33]. The complete body parameters are shown in Figure A8 of the Appendix.

The tire block emulates a tire via a "magic formula" of MATLAB that is based on empirical data using four coefficients to describe tire behavior. The model considers factors such as the "longitudinal" direction of the tire. In other words, the direction in which the tire rolls (in our case, forward only). The simulation has the capacity for more realism as one can implement properties such as compliance (tire flexion), inertia, rolling resistance, and much more. For this simulation purposes, the default settings suffice.

2.3.3 Simulation Scenarios and Results

Scenario 1:

In this scenario we ran the powertrain model with a simple acceleration, stop, and deceleration, as shown in Figure A5 of Appendix. The scenario follows the approximate weight of a semi-truck of 16,000kg without a load, [34]. The speed behavior of the truck model is presented in Figure 7. The power supplied by the engine and the battery is shown in Figure 4.

From Figure 7, it took approximately 15 seconds for the vehicle to reach 100 kph (62 mph). The time it takes for an 18-wheeler to accelerate to 60 mph or decelerate to 0 mph from 60 mph can vary based on several factors such as the truck's weight, engine power, road conditions, and driver behavior.

Generally, a fully loaded 18-wheeler truck might take around 30-60 seconds to accelerate from 0 to 60 mph under normal driving conditions. When it comes to deceleration, again, it depends on various factors including braking system efficiency, road conditions, and the driver's braking habits. Decelerating from 60 mph to 0 mph might take a similar amount of time, typically around 30-60 seconds under controlled braking, [35].

The acceleration time of the truck model (15s from zero to 62mph) may be explained by the fact that it has no load. Figure 7 also shows that the truck model follows the speed command closely.

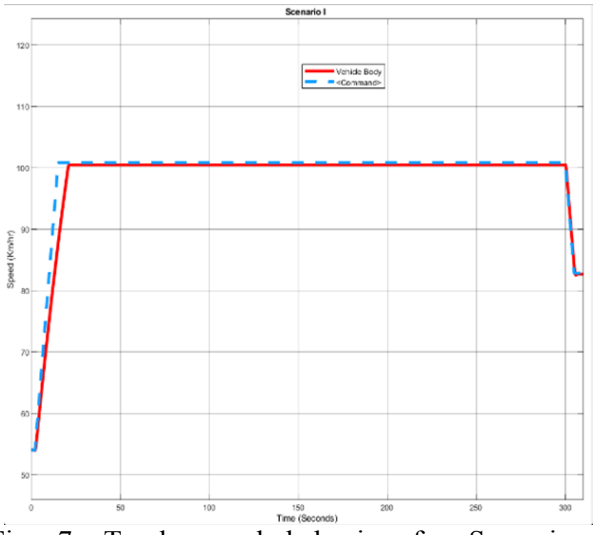

Fig. 7: Truck speed behavior for Scenario 1
Red solid =Vehicle body; Blue dotted= Speed command

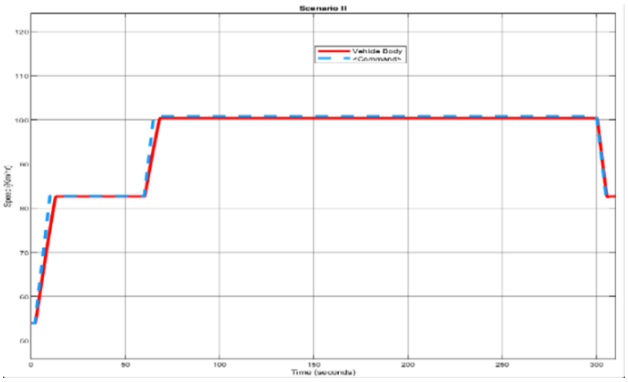

Fig. 8: Truck speed under highway conditions
Red solid =Vehicle body; Blue dotted= Speed command

Scenario 2:
The second simulation scenario follows the speed command for highway conditions in Figure A6 of the Appendix. It uses the approximate weight of a semi-truck of 16,000 kg without a load. The speed behavior of the truck model is shown in Figure 8.

From Figure 8, it took approximately 10 seconds for the vehicle to reach 80 kph (49 mph). Next, the vehicle stops accelerating and then accelerates to 100 kph or 62 mph before beginning deceleration. Again, the truck model follows the speed command closely.

Overall, the simulation results show that the truck model behaves appropriately.

3 Regenerative Braking

3.1 Background

Regenerative braking is a mechanism used in many vehicles to recover the energy that would otherwise be lost during braking. When a vehicle equipped with a regenerative braking system decelerates or brakes, the electric motor functions as a generator and converts the kinetic energy of the vehicle into electrical energy to charge its battery, [36].

The electrical machine then transitions back to motor mode when the driver accelerates the vehicle. Regenerative braking is commonly used in hybrid vehicles, electric vehicles, and some electric bicycles.

Nowadays, the automotive industry is utilizing new electrical systems more than ever to offer advantages such as energy efficiency, improved range, and integration of more sustainable and environmentally friendly transportation systems. This is strongly influenced by the EPA's proposal "to reduce greenhouse gas emissions from heavy-duty vehicles by 2027", [37].

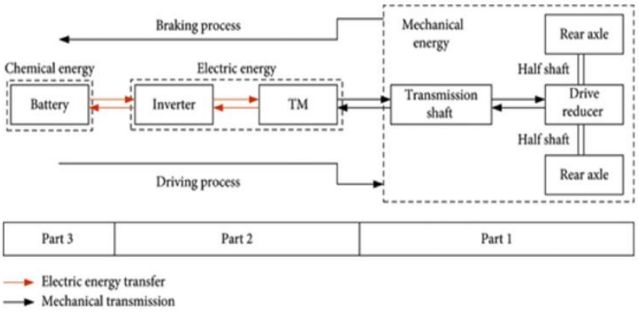

Fig. 9: Regenerative braking diagram, [38]

The implementation of regenerative braking has greatly increased the fuel economy of any vehicle that is integrated with the braking system. For example, the braking system "can reduce the wasted energy up to 8%-25%," resulting in greater mileage for the car, [39]. Notably, the focus is directed toward alternatives that will reduce gas emissions and obtain longer mile ranges. A regenerative braking diagram is shown in Figure 9.

3.2 Specification

With the growing technology and the government desire to push for a greener society, the implementation of these systems is optimal for automotive. In the proposition of an idea, due to semi-trucks often carrying substantial loads and covering long distances, resulting in significant energy expenditure during braking, the development of a fuel-economic semi-truck would be of great benefit in reducing fuel consumption and emissions. As stated earlier, a semi-truck must have a maximum load of 80,000lbs (about 36287kg). Therefore, there is a great amount of wasted energy from the numerous extra trips semi-trucks travel around the country. When put into the application, the following parameters need to be considered:

a) *Kinetic energy:* The kinetic energy, *KE*, of a moving vehicle which estimates the amount of energy available for recovery during braking, which depends on the vehicle weight, *m*, and its speed, *v*, squared, [40].

$$KE_i = KE_f \rightarrow \frac{1}{2}mv_i^2 = \frac{1}{2}mv_f^2 \qquad (1)$$

b) *Energy conversion efficiency:* The energy conversion efficiency determines how effectively the kinetic energy is converted into electrical energy and stored in the battery. It is calculated as the ratio of the electrical energy output to the kinetic energy input, expressed as a percentage, [41].

$$Efficiency = \frac{Electrical\ energy\ output}{Kinetic\ energy\ input} \times 100\% \quad (2)$$

c) *Energy storage capacity:* The energy storage capacity of the battery determines the amount of electrical energy that can be stored for later use. It is typically measured in kilowatt-hours (kWh). This estimates the potential amount of energy that can be stored during regenerative braking, [42].

$$Storage\ Capacity = Battery\ Capacity \times Battery\ Voltage \quad (3)$$

However, it is important to note that the actual amount of energy recovered through regenerative braking depends on various factors, such as the efficiency of the regenerative braking system, the driving conditions, the driver braking behavior, and the overall design and engineering of the vehicle.

The system is best at use in larger speed differences rather than small ones (one being stop and go traffic). Additionally, the efficiency rate of conversion from system to battery, shown by simulation of a "hydraulic hybrid system under mild braking" is 36.93% and 25.28%, [9]. Thus, regenerative braking is very situational and relies on the driver for its full capability in decisions of coasting versus regeneration; although if utilized properly such as in modes of downhill driving, the regeneration amount may be large.

Overall, regenerative braking is a great component in the right direction in increasing MPG or MPGe but is not the main power source of the system. Every semi-truck with the capability to regenerate a large portion from their long mileage trips back will result in longer mileage.

3.3 Representation of Regenerative Braking

For emulating regenerative braking power to the entire hybrid semi-truck system, the level of logic is displayed at a high level. The energy captured in the regenerative braking mode from the semi-truck is modeled through an external power source. An external power source is a battery block model on Simulink that is set at a constant energy level and consists of two output logic states.

The battery model will enter either the dissipation state where it begins feeding energy to the electric motor or a neutral state where the battery is not dissipating at all. These states are monitored by the overall control system of the semi-truck.

4 Solar PV System for Increasing the Range of the Truck Model

4.1 Background and Sizing

In recent years, as the efficiency of solar panels increases and the cost of renewable energy goes down, there have been attempts to utilize this technology for more applications, [43]. One such application is that of a solar-powered vehicle or a vehicle utilizing solar. While solar power has not been able to provide enough energy to power an entire modern electric car, they have been implemented in charging stations and within vehicles to assist in power generation, [16]. Solar power has been utilized in small-scale experimental designs such as solar-powered golf carts and small town-cars for short-distance residential and recreational travel, [44].

Semi-trucks are an important part of the transportation industry and utilize large containers to transport their cargo; these containers can be up to 8 feet tall, 8 feet wide, and 53 feet long making them prime real estate for a large solar array, [34].

For our truck design, 320W Residential Monocrystalline solar panels were used for calculations and simulation. These solar panels provide a solar cell efficiency of 21% and are relatively light compared to the truck and cargo, weighing only 39.7 pounds for a panel 65 inches tall and 40 inches long, [45]. The size of the trailer allows for 18 panels, in two rows of 9, to be placed on each side of the container giving a total power rating of 17.28kW across the 54 panels.

The irradiance received, and thus the output of a solar panel is highly dependent on its topographical location and the weather conditions around it as well as its orientation, [46]. For initial design and calculation, the State of California was used for determining solar resources. On average, throughout the year, California receives about 5.38 peak sun hours or around 5380 Whm^2 per day, [47]. The total kWh energy output of the panels is derived from the equation in [46]:

$$E = A \times r \times H \times PR \quad (4)$$

where:

A is the area of the panel(m^2),
r is the solar panel yield or module efficiency (%),
H is the average solar irradiation on the panels (kWh/m^2), and **PR** is the performance ratio or coefficient for losses, [46].

The result of this equation gives the energy output of each panel at its optimal tilt angle for maximizing annual energy output, which is equal to the latitude of the location where the panel is placed. However, the panels on the semi-trailer are stuck at a fixed angle of either 0° on the top or 90° on the sides.

Using data from the National Renewable Energy Laboratory System Advisor Model (SAM), the panels on the top of the trailer experience a 12-13% loss in energy output while the panels on the sides experience a 20-80% loss in performance depending on their orientation, [47]. Panels facing north receive very little direct sunlight and mostly rely on diffuse radiation to generate energy. If the semi-truck drives east-west an equal amount that it drives north-south the total average output of all the solar panels is around 65.9kWh, peaking during the summer months.

The amount of energy generated by the solar panels is not enough to charge the vehicle on its own but can be used to extend range as well as provide power to auxiliary systems such as the trailer lift or refrigeration. The output voltage of each chosen solar panel is around 33 volts and needs to be increased to a value sufficient to charge the vehicle battery, [45]. There are a total of 54 panels, 18 on each side in 6 rows of 9. Each row is connected in series to the row next to it and then connected in parallel to the other sides, providing a total dc voltage of around 594V, enough to charge the battery.

4.2 Simulation of Solar PV System Design

System representation and simulation setting

We simulate the basic setup of our solar PV system using MATLAB Simulink Simscape toolbox. To simulate the solar panels on the truck we used the relatively simple "PV Array" block. The model of a PV cell used in the array is shown in Figure 10. This block implements a specified array of photovoltaic modules and outputs a five-element vector of measurements into a display block given input irradiance and temperature. The irradiance was set to 5380 W/m2 and the temperature was set to 25°C per standard test conditions as a good approximation of the area where the panels will be placed.

The MATLAB Simulink implementation of the truck solar system design for testing is shown in Figure A11 of Appendix.

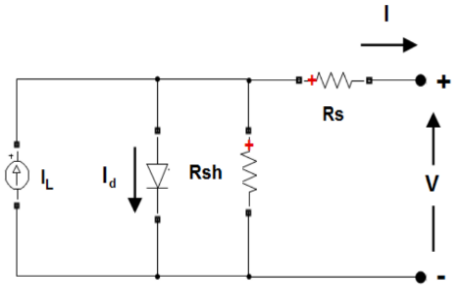

Fig. 10: Solar PV cell model, [48]

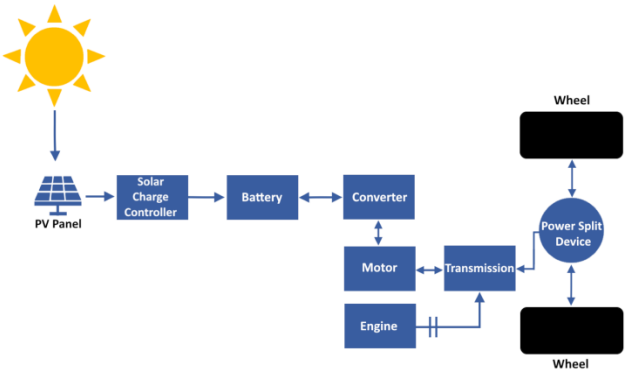

Fig. 11: Complete system block diagram with parallel hybrid drive train configuration

Various parameters are specified within the block such as the number of cells, the optimum operating voltage (Vmp), and the open circuit voltage (Voc). These parameters were obtained from the manufacturer datasheet for the specified panels being tested, [45]. Lastly, the number of modules connected in series per string and the number of parallel strings is specified. With just these two parameters it is not possible to set up a more complicated system, so we still use the 18 modules on each side of the trailer that are connected in series strings before all three strings are connected in parallel.

Results

Using the above parameters the solar model produces an output of 652.7V and 105.2kW dc. After factoring in the loss in performance from the suboptimal orientation of the panels (an average of 39% across the 3 sides) we obtain a power output of 63.82kWh, which is slightly lower than the estimated 65.9kWh from the theoretical calculations. However, the result shows that the simulated model closely imitates the designed solar systems.

5 Complete 18-wheeler Hybrid Electric Vehicle Design

Figure 11 represents a block diagram of the entire vehicle system. Starting with the solar charging of the vehicle, when sunlight falls on the solar panels, they generate electrical energy. The electrical energy produced by the solar panels is sent to the battery through the charge controller unit.

A maximum power point tracker (MPPT) is a charge controller unit that regulates the charging process of the energy storage system, such as batteries. It optimizes the charging parameters to ensure efficient and safe charging. This includes monitoring the battery voltage and current levels, as well as temperature, and adjusting the charging rate accordingly, [49]. The charge controller unit prevents overcharging or undercharging, which can degrade battery life or affect performance, [50].

Power from the panels is dependent on its voltage and the current drawn from the panel. As more current gets drawn, the voltage provided will decrease, and the current-voltage (I-V) curve for a solar panel and other power sources is nonlinear. Due to factors affecting the energy input like temperature and weather, the maximum power point would constantly change. A simple charge controller is implemented for our truck design rather than a more complicated MPPT for cost and safety reasons. There is a DC-to-DC conversion that takes place in the charge controller to regulate the voltage and current going into the battery, [51].

The energy storage system, now charged with solar energy, acts as a reservoir of electrical energy. When needed, the electrical energy from the energy storage system is sent to the electric motor. The electric motor converts the electrical energy back into mechanical power, which is used to drive the wheels of the vehicle and provide propulsion.

One of the main components of an electric vehicle system is the inverter, located between the battery and the electric motor. Its primary function is to convert the DC electrical energy from the battery into AC electrical energy and control the electric motor speed. In our system we implement a bi-directional converter that can run the AC motor as well as turn AC power from regenerative braking into DC to charge the battery, [52].

Moving on to the powertrain and regenerative braking system, when the parallel hybrid vehicle is in operation, the internal combustion engine generates mechanical power. This power is independent of the electrical power produced by the electric generator. Both the mechanical power and the electrical power are combined in a gear system to drive a motor and the wheels.

Regenerative braking helps to recharge the batteries and improve overall efficiency. A power split device is utilized to facilitate the conversion of mechanical energy from the wheels into electrical energy during braking. During deceleration or braking, the electric motor functions as a generator and converts some of the kinetic energy of the vehicle into electrical energy, which is then stored in the battery.

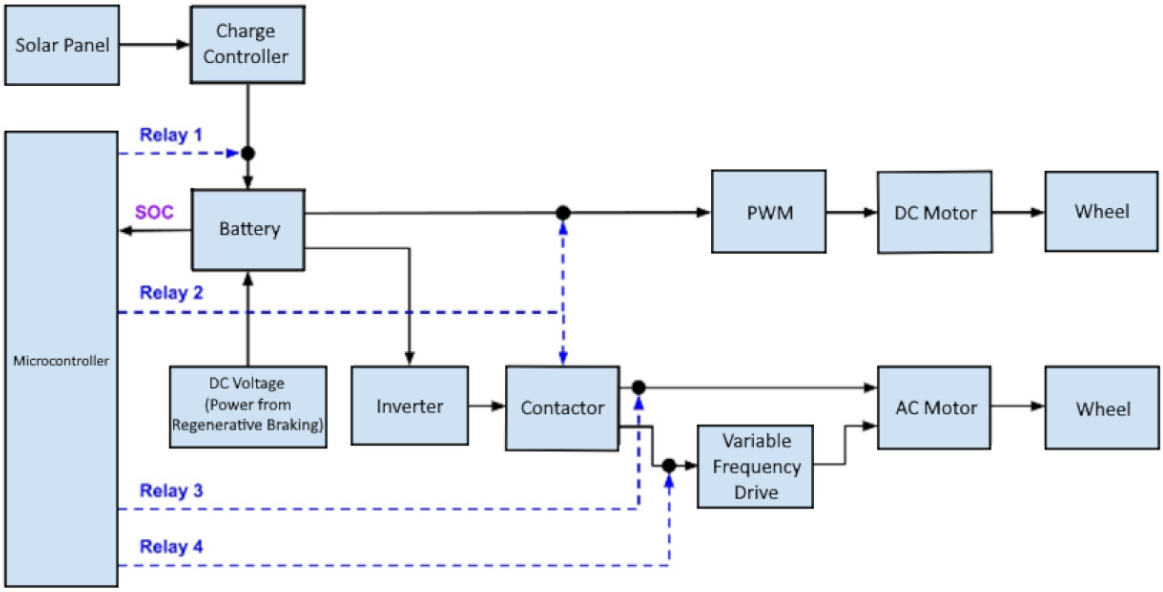

Fig. 12: Block diagram for 18-wheeler hybrid EV prototype (series hybrid drivetrain configuration)
(List of components and specifications are provided in Appendix)

6 Prototype of 18-wheeler Hybrid Electric Vehicle

6.1 Prototype Description and Parameters

Because it is difficult to find a physical gearbox and a diesel engine (Figure 3) we chose to build a prototype using the hybrid series drivetrain, which can be seen in Figure A12 of Appendix.

The prototype block diagram is shown in Figure 12 where small-size components are used to build the truck model. The battery is connected to a microcontroller that monitors its state of charge and controls various relays for charging and outputting power to the motors. The solar system is represented by a single small solar panel that charges the battery via a charge controller. There are two electrical motors (one is AC and the other is DC) which drive two separate wheels. Their speed is controlled by two separate drives (PWM and Variable Frequency Drive-VFD). The AC motor can be run at two different speeds, one is controlled by the inverter frequency and the other is controlled by the VFD. A DC power supply is used to represent the power regained from regenerative braking and the power generated by the diesel engine in the series drivetrain configuration.

The DC motor speed is controlled by a pulse-width modulator (PMW) drive. The PWM takes the battery's constant voltage and outputs it into a square pulse waveform, alternating between intervals of no voltage and the maximum of the input voltage. A potentiometer controls the wave's duty cycle, determining how long the output voltage is set high or low for each period. Higher duty cycles result in higher average output voltage which yields higher DC motor speeds. There is a switch that can reverse the motor's rotational direction by inverting the polarity of the voltage supplied to the motor's terminals.

Using a digital tachometer, the maximum speed of the DC motor was recorded as roughly 400 RPM. Its speed can be adjusted incrementally down to 0 RPM manually by turning a knob off its PMW drive.

A pure sine wave inverter (Figure 12) takes the battery 12-V DC and outputs 120 VAC at 60 Hz. Terminals of the battery are connected to alligator clips on a wire that connects into the input terminals of the inverter with banana plugs. The AC voltage is taken from the inverter's AC socket with a power cord. Since there is a 120-V voltage present, the AC signal needs to be enclosed in an electrical-insulated junction box. The power cord is secured to a contactor in the metal enclosure to avoid injury from electrical shocks and to protect the connections. The hot and neutral wires from the power cord are connected to the two-pole contactor that is normally closed and allows control of the output.

The synchronous speed of an AC motor is only dependent on the number of magnetic poles it has and the frequency of its power supply. Since the number of poles in the motor cannot be feasibly altered, the most optimal way to change the speed of our AC motor (Figure 12) is to change the frequency of the voltage supplied to it. A variable frequency drive (VFD) is the device used to change the 120-V, 60-Hz AC signal into another frequency and voltage while keeping the frequency-voltage ratio the same. We could output a 100-VAC signal at 50 Hz since the output cannot have a higher voltage than the available input. This way, the AC motor can be run at two different speeds.

The physical implementation of the prototype is shown in Figure 13. Its components and specifications are provided in Table 1, Table 2 and Table 3 of the Appendix.

6.2 Software in Prototype

In implementing the different states of the physical system, code logic was programmed into an Arduino Uno R3 microcontroller. The logic flow chart is shown in Figure 14. The relay wiring diagram is provided in Figure 15. The complete code of the microcontroller is provided in Appendix.

The integration of the code in the microcontroller allows the system to automatically determine when to charge or not to charge the battery to prevent over-charging and over-discharging, as well as to operate the motors according to the defined logic.

The basic logic flow for the microcontroller where pieces of the code are taken from a project on a solar tent designed for outdoor living that also implements a state of charge sensor for its battery, [53].

When the microcontroller reads the battery voltage the code then calculates for state of charge (SOC). A voltage divider segments the battery voltage for the microcontroller. ADC reads 0-5V (0-1024 values), correlated with the battery discharge curve in Figure A13. At 13.8V, ADC 900 means 100% SOC. Mapping, done without load, faces accuracy challenges under load or while charging, with a ±5% error. Non-linear discharge curves complicate precision.

These calculations are then displayed on the LCD screen. From this SOC calculation, if the SOC is below a certain threshold of 30% the system is not allowed to run. Otherwise, the system will continue

with the system logic. The logic then proceeds to a switch that determines how fast the rotation of the AC motor will be. When the switch logic is high, the AC motor's rotation is at 50Hz, while toggled off it is at 60Hz. Several LED are used to indicate different operation conditions of the prototype.

6.3 Testing of Prototype

Testing shows that the prototype works properly. The AC motor can be run at two different speeds while the DC motor speed can be regulated. Figure 16 and Figure 17 show the supply voltage to the DC motor at 90% and 100% speed.

The transitions of the microcontroller logic (Figure 14) are verified by artificial changing of the battery SOC. These tests show that the transitions follow the defined logic, as shown by the LED indicators.

6.4 Project Cost

In total, around $835 USD was put into creating the physical model with $580 spent on the final design components and the rest spent on components that either were not implemented or did not work as intended. In addition, a truck model (Yellow, Figure 13) was purchased for $80, but this was purely for representational and aesthetic purposes. The full list of parts and costs is provided in Table 1 of the Appendix.

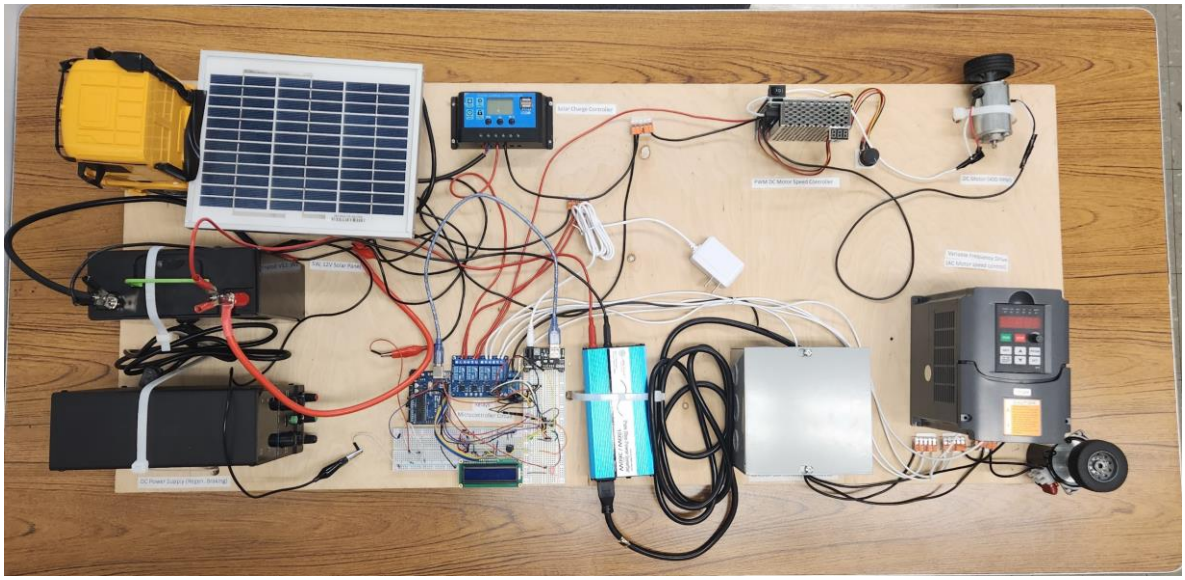

Fig. 13: Prototype of 18-wheeler hybrid electric vehicle

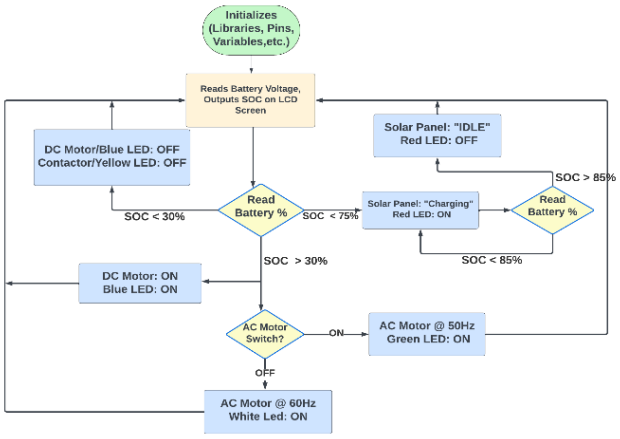

Fig. 14: Microcontroller logic flow

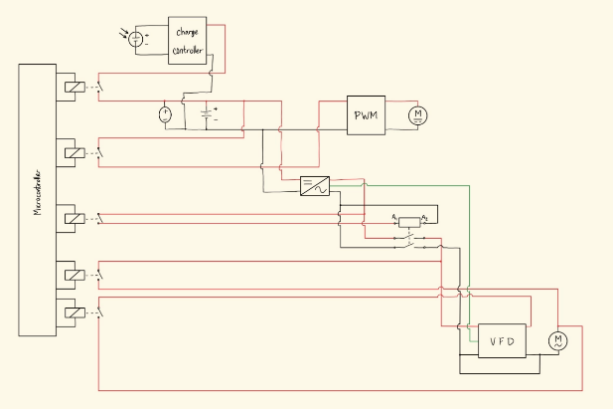

Fig. 15: Microcontroller and relay wiring diagram

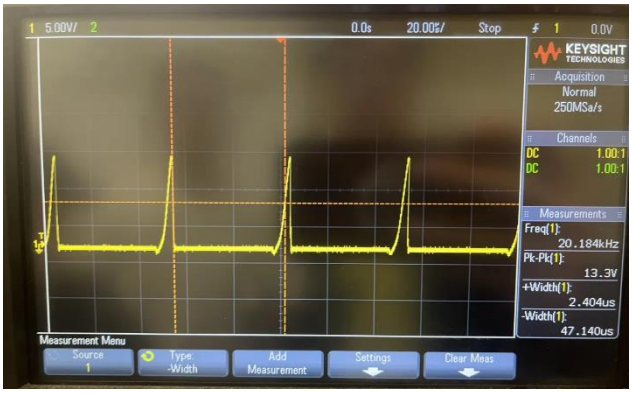

Fig. 16: Supply voltage for DC motor at 90% speed

Fig. 17: Supply voltage for DC motor at 50% speed

6.5 Troubleshooting and Lessons Learned

Technical rectification

The initial design of the project followed a series of hybrid drivetrain configurations, but throughout simulation a parallel configuration was chosen. However, for implementation of the prototype we had to use the series hybrid drivetrain configuration due to difficulty in finding a suitable physical diesel engine and a gearbox.

The project required multiple tests and changes for all the components to function entirely. The complications occurred mainly in the components connected to the AC motor. Commonly during testing, parts such as the variable frequency drive (VFD) would not function properly. A multimeter is used to find where in the line any issues would occur.

After many tests, inconsistencies in the variable frequency drive operating resulted from loose connections in the contactor. We resolved this issue by screwing down all wires going in and out of the contactor to provide more reliable contacts for the VFD to be powered.

Another common problem is that the AC motor would not operate smoothly at different speeds. We tested the AC motor to be supplied over a range of different frequencies and could not get the motor to run smoothly or at all at times. We decided to run the motor's alternate speed with a supply frequency of 50 HZ at 100 volts to maintain the voltage-frequency ratio constant while not deviating far from the rated 60 Hz to avoid burning the motor while still controlling its speed.

Various control changes were also made to better facilitate the desired function. The microcontroller monitors the SOC in the battery and controls whether power can be output to the motors or not. When the battery power reached near the threshold of turning the motors off it would constantly flip on and off due to the slight inaccuracy of the sensor and noise voltages. This issue was fixed by adding a longer delay between SOC checks so that it would only turn off/on if the voltage was constant over a relatively long period. A switch was also added to control the speed of the AC motor to make it more stable and more like the pedal in a car.

The initial design of the physical prototype did not include enough safety measures and controls such as the use of relays and the junction box for the AC signal. Initially, some 18-awg wire was used for some connections which could have caused injury and connection failure as wires overheated or melted so this wire was changed to 14-awg later in the project. Some parts like the VFD did not work well initially and had to be troubleshooted and limited in function to perform the desired task. Better quality VFDs were cost-prohibitive as were larger motors and controllers.

Teamwork experience

Throughout our project teamwork and the separation of duties were imperative to hitting the appropriate deadlines where one team working on the simulation and another working on the physical implementation. In large teams, it is often difficult to get everyone on the same page and to work in large groups that fit everyone's schedules. Working in small parts, keeping regular notes, and bringing the parts together once each is complete are important steps in working on a team. It is also important to ask for and accept any genuine critiques and feedback about a design or implementation to make it better.

7 Conclusion

In the pursuit of creating an innovative hybrid semi-truck (18-wheeler) model, this project integrates simulation and physical implementation, providing a comprehensive exploration of the system's design, functionality, and performance. The hybrid semi-truck model is conceived with a focus on enhancing

range and energy efficiency by utilizing regenerative braking, solar power, and a microcontroller-based control system. The project outcomes are summarized as follows.

a) The novel features of the truck design include using 60% electric power and only 40% diesel, and range extension using regenerative braking and solar PV, which is partially implemented in the prototype.
b) Simulation of the electric 18-wheeler design using MATLAB Simulink shows that the model works properly. It follows the speed command closely. Its acceleration and deceleration behaviors are normal and its acceleration time is reasonable.
c) The truck prototype, constructed with a DC motor and an AC motor as the vehicle drives, presented a real-world embodiment of the simulated design. The prototype control is mostly automatic, which is performed by a microcontroller, motor speed drives, and multiple relays.
d) Testing of the prototype shows that it functions accurately. The DC motor speed can be regulated over a wide speed range while the AC motor can run at two different speeds as designed. The microcontroller logic is followed, ensuring the safe operation of the solar PV system, the battery, and appropriate control of the motors.

Overall, the hybrid semi-truck project succeeded in achieving a harmonious blend of simulation, design, and physical implementation. It can be used as an engineering and public education tool on electric vehicle subject. Furthermore, by exploring cutting-edge technologies such as regenerative braking and solar power for truck range extension, the project contributes to enhancing vehicle efficiency and finding sustainable transportation solutions, which make the transportation sector friendlier to the environment.

References:

[1] United States Environmental Protection Agency, "Fast Facts on Transportation Greenhouse Gas Emissions." EPA, [Online]. https://www.epa.gov/greenvehicles/fast-facts-transportation-greenhouse-gas-emissions (Accessed Date: October 12, 2023).

[2] G. Sharkey, "What is the carbon footprint of a truck?." FreightWaves, 2021, [Online]. https://www.freightwaves.com/news/what-is-the-carbon-footprint-of-a-truck (Accessed Date: October 12, 2023).

[3] P. Cohen, "Pros and Cons of Electric and Hybrid Trucking Vehicles." https://ezfreightfactoring.com/blog/electric-and-hybrid-commercial-vehicles/ (Accessed Date: October 12, 2023).

[4] M. D. Meiller, "Five Smart Ways to Improve EV Battery Production," [Online]. https://www.nordson.com/en/about-us/nordson-blog/efd-blogs/five-smart-ways-to-improve-ev-battery-production (Accessed Date: October 12, 2023).

[5] A. Moseman, "Are electric vehicles definitely better for the climate than gas-powered cars?," *MIT Climate Portal*, MIT Climate, [Online]. https://climate.mit.edu/ask-mit/are-electric-vehicles-definitely-better-climate-gas-powered-cars (Accessed Date: November 10, 2023).

[6] M. H. Ullah, T. S. Gunawan, M. R. Sharif, and R. Muhida, "Design of environmental friendly hybrid electric vehicle," in *2012 International Conference on Computer and Communication Engineering (ICCCE)*, 3-5 July 2012 2012, pp. 544-548, doi: 10.1109/ICCCE.2012.6271246.

[7] J. Glueck and H. T. Le, "Impacts of Plug-in Electric Vehicles on local distribution feeders," in *2015 IEEE Power & Energy Society General Meeting*, 26-30 July 2015 2015, pp. 1-5, doi: 10.1109/PESGM.2015.7286348.

[8] "How Regenerative Brakes Work", U.S. Department Of Energy, [Online]. https://www.energy.gov/energysaver/how-regenerative-brakes-work (Accessed Date: November 10, 2023).

[9] T. Liu, J. Jiang, and H. Sun, "Investigation to Simulation of Regenerative Braking for Parallel Hydraulic Hybrid Vehicles," in *2009 International Conference on Measuring Technology and Mechatronics Automation*, 11-12 April 2009 2009, vol. 2, pp. 242-245, doi: 10.1109/ICMTMA.2009.418.

[10] A. Carrillo, A. Pimentel, E. Ramirez, and H. T. Le, "Mitigating impacts of Plug-In Electric Vehicles on local distribution feeders using a Charging Management System," in *2017 IEEE Transportation Electrification Conference and Expo (ITEC)*, 22-24 June 2017 2017, pp. 174-179, doi: 10.1109/ITEC.2017.7993267.

[11] T. Vo, J. Sokhi, A. Kim, and H. T. Le, "Making Electric Vehicles Smarter with Grid and Home Friendly Functions," in *2018 IEEE Transportation Electrification Conference and Expo (ITEC)*, 13-15 June 2018 2018, pp. 183-187, doi: 10.1109/ITEC.2018.8449949.

[12] Grid Deployment Office, "Biden-Harris Administration Announces Up to $3.9 Billion to Modernize and Expand America's Power Grid." United States Department of Energy, [Online]. https://www.energy.gov/gdo/articles/biden-harris-administration-announces-39-billion-modernize-and-expand-americas-power 2023 (Accessed Date: November 10, 2023).

[13] M. Tedesco, "The Paradox of Lithium." Columbia Climate School, 2023, [Online]. https://news.climate.columbia.edu/2023/01/18/the-paradox-of-lithium/ (Accessed Date: November 10, 2023).

[14] V. Keseev, "Efficiency Improvement of Electric and Hybrid Vehicles by Better Utilization of Inertia," in *2022 8th International Conference on Energy Efficiency and Agricultural Engineering (EE&AE)*, 30 June-2 July 2022 2022, pp. 1-5, doi: 10.1109/EEAE53789.2022.9831301.

[15] E. C. Evarts, "Lithium batteries: To the limits of lithium," *Nature*, vol. 526, no. 7575, pp. S93-S95, 2015/10/01 2015, doi: 10.1038/526S93a.

[16] Toyota, "Prime Time for More EV Miles with the All-New 2023 Prius Prime." Toyota. 2023.

[17] California Air Resources Board, "Zero-Emission On-Road Medium-and Heavy-Duty Strategies", [Online]. https://ww2.arb.ca.gov/resources/documents/zero-emission-road-medium-and-heavy-duty-strategies (Accessed Date: November 12, 2023).

[18] Z. Syed, S. A. Singh, S. Venkateswaran, and A. Bandiwdekar, "Hybrid engine," *2015 International Conference on Technologies for Sustainable Development (ICTSD)*, pp. 1-5, 2015.

[19] California Air Resources Board, "Advanced Clean Trucks." CARB, [Online]. https://ww2.arb.ca.gov/our-work/programs/advanced-clean-trucks (Accessed Date: November 12, 2023).

[20] U.S. Department of Energy, "Where the Energy Goes: Hybrids", [Online]. https://www.fueleconomy.gov/feg/atv-hev.shtml c.

[21] J. Stinson, "Why hybrid diesel trucks never quite caught on." Trucking Dive, [Online]. https://www.truckingdive.com/news/hybrid-diesel-class-8-truck-long-haul/596782/ 2021 (Accessed Date: November 12, 2023).

[22] M. Gokasan, S. Bogosyan, and D. J. Goering, "A diesel engine map model based observer for HEVs," in *2005 IEEE Vehicle Power and Propulsion Conference*, 7-7 Sept. 2005 2005, pp. 545-550, doi: 10.1109/VPPC.2005.1554591.

[23] V. Sreedhar, "Plug-In Hybrid Electric Vehicles with Full Performance," in *2006 IEEE Conference on Electric and Hybrid Vehicles*, 18-20 Dec. 2006 2006, pp. 1-2, doi: 10.1109/ICEHV.2006.352291.

[24] N. Penina, Y. V. Turygin, and V. Racek, "Comparative analysis of different types of hybrid electric vehicles," in *13th Mechatronika 2010*, 2-4 June 2010 2010, pp. 102-104.

[25] J. Alien, "How Much Torque Does a Semi Truck Have: Unveiling the Power within." Road Rize, 2023, [Online]. https://roadrize.com/how-much-torque-does-a-semi-truck-have/ (Accessed Date: November 20, 2023).

[26] A. Du, X. Yu, and J. Song, "Structure design for power-split hybrid transmission," in *2010 IEEE International Conference on Mechatronics and Automation*, 4-7 Aug. 2010 2010, pp. 884-887, doi: 10.1109/ICMA.2010.5589018.

[27] Inch Calculator, "Horsepower to Watts Converter." Inch Calculator, [Online]. https://www.inchcalculator.com/convert/horsepower-to-watt/ (Accessed Date: November 20, 2023).

[28] MathWorks, "Parallel Hybrid Transmission." MathWorks, 2023, [Online]. https://www.mathworks.com/help/sdl/ug/parallel-hybrid-transmission.html (Accessed Date: November 20, 2023).

[29] Electrical4U, "Ohm's Law: How it Works (Formula and Ohm's Law Triangle)", 2022, [Online]. https://www.electrical4u.com/ Accessed Date: November 20, 2023).

[30] X. Zhang, J. Hou, Z. Wang, and Y. Jiang, "Study of SOC Estimation by the Ampere-Hour Integral Method with Capacity Correction Based on LSTM," *Batteries*, vol. 8, no. 10, p. 170, 2022, [Online]. https://doi.org/10.3390/batteries8100170.

[31] L. Timilsina, P. R. Badr, P. H. Hoang, G. Ozkan, B. Papari, and C. S. Edrington, "Battery Degradation in Electric and Hybrid Electric Vehicles: A Survey Study," *IEEE Access,* vol. 11, pp. 42431-42462, 2023, doi: 10.1109/ACCESS.2023.3271287.

[32] M. Gudino, "Types of Switching DC to DC Converters", 2017, [Online]. https://www.arrow.com/en/research-and-events/articles/types-of-switching-dc-dc-converters (Accessed Date: November 20, 2023).

[33] Caltrans, "Legal Basis for Truck Restrictions." California Department of Transportation, [Online]. https://dot.ca.gov/programs/traffic-operations/legal-truck-access/legal-basis-truck-restrictions (Accessed Date: November 20, 2023).

[34] Transwest Trailers, "Semi Trailer Dimensions, Length & What Can You Haul." Transwest Trailers, 2021, [Online]. https://www.transwest.com/trailers/blog/semi-trailer-dimensions-length-and-what-can-you-haul/ (Accessed Date: November 20, 2023).

[35] P. Bokare and A. Maurya, "Acceleration-Deceleration Behaviour of Various Vehicle Types," *Transportation Research Procedia,* vol. 25, pp. 4737-4753, 07/31 2017, doi: 10.1016/j.trpro.2017.05.486.

[36] J. S. Choksey, "What is Regenerative Braking?", 2021, [Online]. https://www.jdpower.com/cars/shopping-guides/what-is-regenerative-braking (Accessed Date: November 20, 2023).

[37] United States Environmental Protection Agency, "Regulations for Greenhouse Gas Emissions from Commercial Trucks & Buses." EPA, 2023.

[38] Y. Xiong, Q. Yu, S. Yan, and X. Liu, "An Innovative Design of Decoupled Regenerative Braking System for Electric City Bus Based on Chinese Typical Urban Driving Cycle," *Mathematical Problems in Engineering,* vol. 2020, p. 8149383, 2020/07/18 2020, doi: 10.1155/2020/8149383.

[39] F. Wang, X. Yin, H. Luo, and Y. Huang, "A Series Regenerative Braking Control Strategy Based on Hybrid-Power," in *2012 International Conference on Computer Distributed Control and Intelligent Environmental Monitoring*, 5-6 March 2012 2012, pp. 65-69, doi: 10.1109/CDCIEM.2012.22.

[40] K. Nice, "How Force, Power, Torque and Energy Work", [Online]. https://auto.howstuffworks.com/auto-parts/towing/towing-capacity/information/fpte9.htm (Accessed Date: November 20, 2023).

[41] "Efficiency", Energy Education, [Online]. https://energyeducation.ca/encyclopedia/Efficiency (Accessed Date: November 15, 2023).

[42] pveducation.org, "Battery Capacity", [Online]. https://www.pveducation.org/pvcdrom/battery-characteristics/battery-capacity (Accessed Date: November 15, 2023).

[43] Renogy, "*How Solar Panels and Solar Energy Have Evolved Over the Past 5 Years*", 2022, [Online]. https://www.renogy.com/blog/how-solar-panels-and-solar-energy-have-evolved-over-the-past-5-years/ (Accessed Date: February 23, 2024)

[44] E. S. H. Mak, "Solar Town Car Development Programme," in *2020 8th International Conference on Power Electronics Systems and Applications (PESA)*, 7-10 Dec. 2020 2020, pp. 1-4, doi: 10.1109/PESA50370.2020.9343959.

[45] Renogy, "RNG-320D Datasheet." Renogy, [Online]. https://www.renogy.com/content/RNG-320D/320D-Datasheet.pdf (Accessed Date: November 15, 2023).

[46] J. P. Dunlop, *Photovoltaic Systems*, 3rd ed. 2012.

[47] "System Advisor Model Version 2022.11.29." National Renewable Energy Laboratory, 2022, [Online]. https://sam.nrel.gov/citing-sam.html (Accessed Date: November 15, 2023).

[48] MathWorks, "PV Array - MATLAB & Simulink." MathWorks. 2023.

[49] MathWorks, "MPPT Algorithm," vol. 2024, [Online]. https://www.mathworks.com/ (Accessed Date: November 15, 2023).

[50] C. P. S. Allen, "Solar Charge Controllers: What Are They and How Much Do They Cost?", Forbes, [Online]. https://www.forbes.com/home-improvement/solar/solar-charge-controllers/ (Accessed Date: November 15, 2023).

[51] A. S. Samosir, S. Purwiyanti, H. Gusmedi, and M. Susanto, "Design of DC to DC Converter for Solar Photovoltaic Power Plant Applications," in *2021 International Conference on Converging Technology in Electrical and Information Engineering (ICCTEIE)*, 27-28 Oct. 2021 2021, pp. 132-137, doi: 10.1109/ICCTEIE54047.2021.9650639.

[52] A. Mohamed, M. Elshaer, and O. Mohammed, "Bi-directional AC-DC/DC-AC converter for power sharing of hybrid AC/DC systems," in *2011 IEEE Power and Energy Society General Meeting*, 24-28 July 2011 2011, pp. 1-8, doi: 10.1109/PES.2011.6039868.

[53] D. C. A. Sacks, J. S. Cucal, Alan Dai, Alvin Dai, S. Elias, J. Godinez, J. Jaurigue, K. Nguyen, H. Vargas, Ha Thu Le,, "Solar Powered Tent for Comfortable Outdoor Living, Emergency and Flexible Activities," *International Journal of Renewable Energy Sources*, vol. 9, 2023.

[54] NERMAK, "12V 20Ah Lithium Iron Phosphate Battery", [Online]. https://www.amazon.com/NERMAK-Phosphate-Rechargeable-Lighting-Scooters/dp/B0B6ZBZ8T7?th=1 (Accessed Date: November 15, 2023).

[55] AIMS Power, "DC to AC pure sine power inverter PWRI18012S instruction manual", [Online]. AIMS Power. aimscorp.net, 2018 (Accessed Date: October 12, 2023).

[56] "LiFePO4 Battery Discharge and Charge Curve." BravaBattery, [Online]. https://www.bravabatteries.com/lifepo4-battery-discharge-and-charge-curve/ (Accessed Date: November 15, 2023).

APPENDIX

Table 1. List of components and costs

Description	Quantity	Cost, $USD
NERMAK 12V 20Ah Lithium LiFePO4 Deep Cycle Battery	1	79.99
Elegoo uno R3 microcontroller	1	29.99
14 Gauge Primary Wire	4	27.99
Contactor	2	19.99
5W 12V Solar Panel	1	28.99
60 Hz AC motor	1	24.99
SunFounder Lab 4 Relay Module 5V	1	7.99
AIMS 180-WATT Pure Sine Inverter	1	86.00
5-wire lever nut	10	7.99
Power cord	1	6.99
DC motor (not used)	1	20.25
DC motor/generator	1	26.99
Junction box	1	34.99
Depvko Solar Charge Controller	1	11.99
Truck Model	1	79.99
Battery Charging Control Board (not used)	1	8.99
Motor controller (not used)	1	11.50
DC Motor speed controller	1	20.99
Lithium Battery Charger	1	27.99
DC power supply	1	57.99
Huanyang Variable Frequency Drive (VFD)	1	139.99
Battery Cables	2	7.99
TOTAL (Including Taxes and Shipping)		**$ 835.60**

Table 2. Lithium LiFePO4 battery specification, [54]

Characteristic	Details
Battery Type	Lithium Ion
Cycle Life	>2000 cycle
Rated Capacity	20 Ah (0.2C,25°C)
Voltage	12.8 V
Wattage	255 W
Weight	5.5 LB
Charging Voltage	14.6±0.2V
Dimensions	(L x W x H): 7.16 x 6.69 x 3.03 inches
Continuous Discharge Current	20A
Continuous Charge Current	12A
Operating Temperature	Discharging: -4°F to 140°F; Charging: 32°F to 113°F
Peak discharge current	60A (Duration: less than 5 seconds)

Table 3. Inverter specifications, [55]

Characteristic	Details
Model NO	PWR18012S
DC Input Voltage	12V (10-16V)
Output Wave Form	Pure Sine Wave THD <3%
Output Power	180W
Surge Power Capacity	360W for 40 milliseconds
Efficiency	Over 90%
No Load Current	0.4A
Battery Low Alarm	DC 9.8 +/- 0.3V
Battery Low Shutdown	DC 9.5 +/- 0.5V
Input Over Voltage Shutdown	16 +/- 0.5 VDC
Operating Temperature (Automatic Recovery/Shutdown)	32-113° F
Over Temperature Protection	149° F +/- 8° F
FAN	Load based
Marine	Conformal coated to protect again moisture and corrosion
USB Output	5 VDC, Max 1A
Internal DC Input	Fuse Must Be Fitted, Use 30A
Remote Switch Port	Yes
Recommended Cable Size	20 AWG or bigger
Mounting Hole Location	3 5/8” hole to hole on width side
Power Switch	ON/OFF Control
Cigarette Lighter Cable	Yes
Dimensions (LxWxH)	6.75” x 3.25” x 1.5”
Net Weight	1 lb

A. Simulation blocks

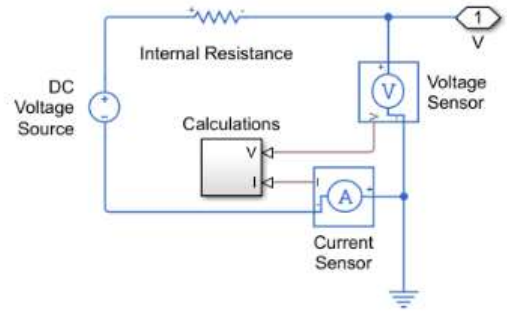

Fig. A1: Inside simulation Battery block

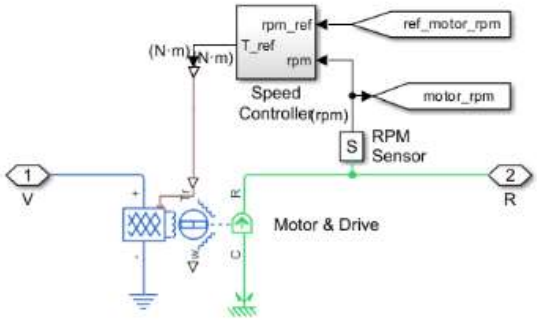

Fig. A2: Inside the simulation Motor block

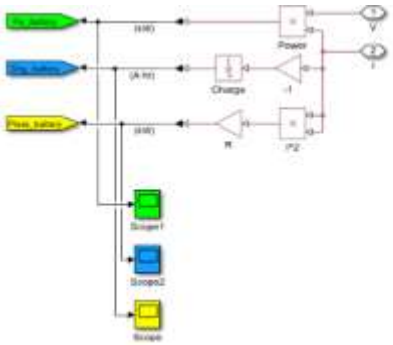

Fig. A3: Calculations from battery voltage and current

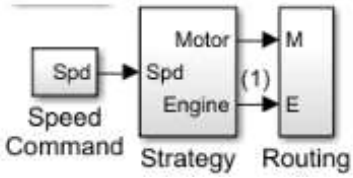

Fig. A4: Blocks for creating vehicle speed command

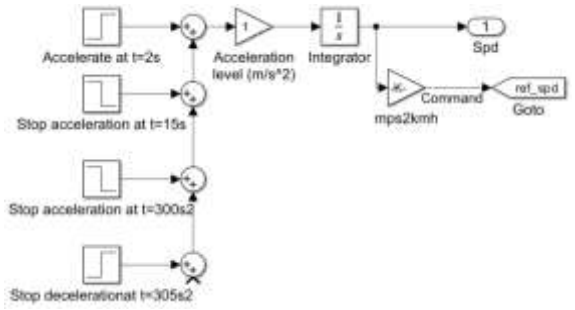

Fig. A5: Inside the Speed Command block

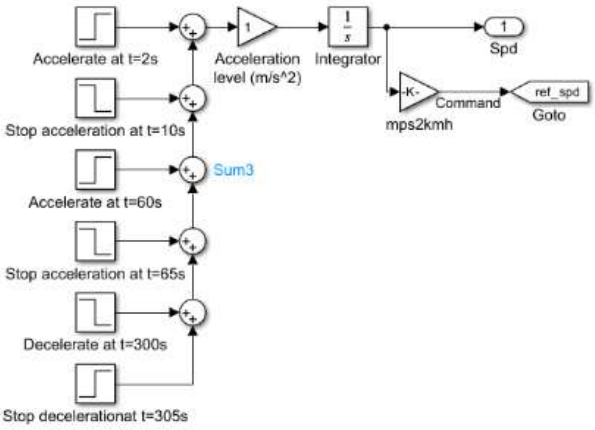

Fig. A6: Speed command for Highway conditions

Fig. A7: Generic engine specification

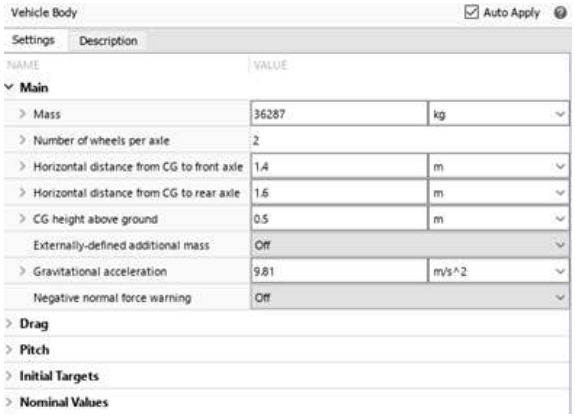

Fig. A8: Vehicle body specification

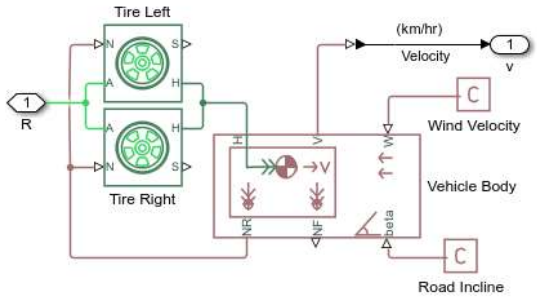

Fig. A9: Tire block configuration

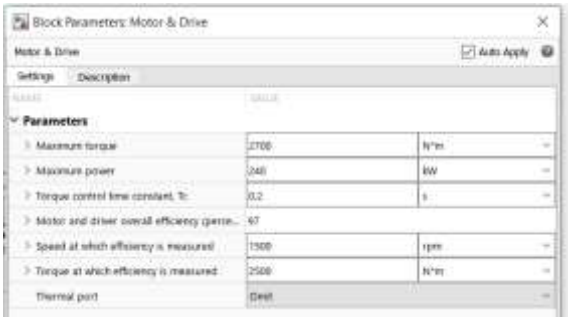

Fig. A10: Motor and Drive block parameters

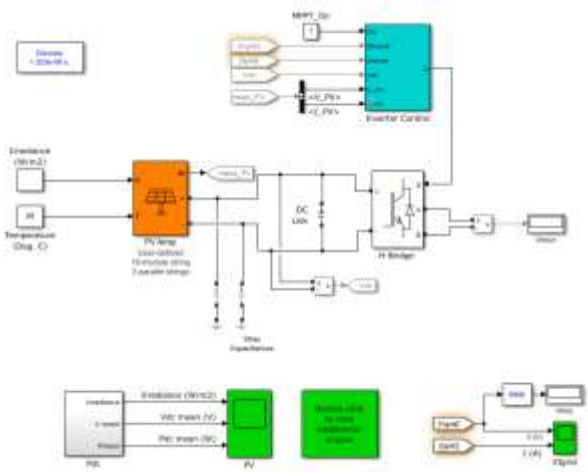

Fig. A11: MATLAB Simulink implementation for testing truck solar PV system design

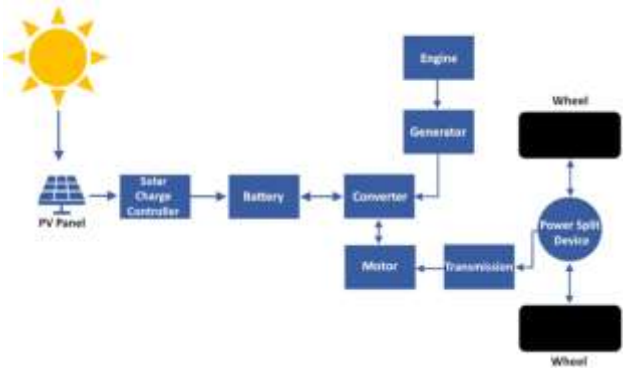

Fig. A12: Complete 18-wheeler block diagram with series hybrid drive train configuration

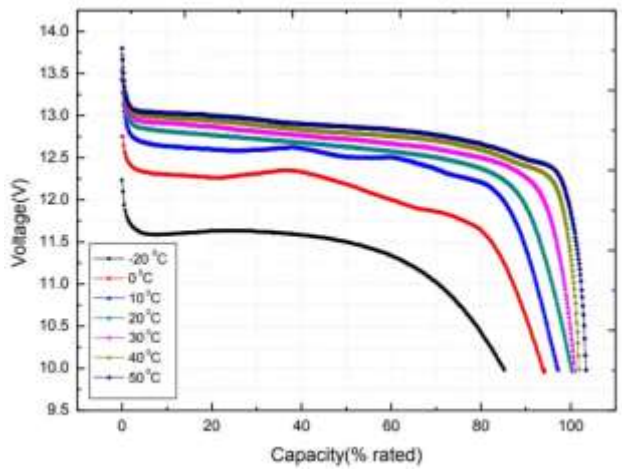

Fig. A13: LiFePO4 battery discharge curve, [56]

B. Arduino code

```
#include <LiquidCrystal.h>
#include <ezButton.h>
ezButton toggleSwitch(13);
LiquidCrystal lcd(7, 8, 9, 10, 11, 12);

double SOC = 0.05;
int SOC_Value = 0;
int bat_percent = 0;
String Status = "Charging";
const int RELAY_1 = 5; // Solar Panel
const int RELAY_2 = 4; // DC Motor/
const int RELAY_3 = 3; // AC Motor @ 60 Hz
const int RELAY_4 = 2; // AC Motor @ 50 Hz
const int RELAY_5 = 6; // Contractor
const int ADC_READ = A5; // reads the battery
void setup()
{
 Serial.begin(9600);
 toggleSwitch.setDebounceTime(100);
 pinMode(ADC_READ, INPUT);
 pinMode(RELAY_1, OUTPUT);
 pinMode(RELAY_2, OUTPUT);
 pinMode(RELAY_3, OUTPUT);
 pinMode(RELAY_4, OUTPUT);
 pinMode(RELAY_5, OUTPUT);
 digitalWrite(RELAY_1, LOW); // Normally Open
 digitalWrite(RELAY_2, LOW); // Normally Open
 digitalWrite(RELAY_3, LOW); // Normally Open
 digitalWrite(RELAY_4, HIGH); // Normally Open
 digitalWrite(RELAY_5, LOW); // Normally Open
 lcd.begin(16,2); //INIT
 }


void loop(){
  Beginning();
  delay(1000);
 if (bat_percent >= 80){
  Status = "Idle";
  digitalWrite(RELAY_1, HIGH); }

 if (bat_percent < 75){
  Status = "Charging";
  digitalWrite(RELAY_1, LOW); }

 if (bat_percent > 30){
  switch_motor(); }

 if (bat_percent < 30){
    digitalWrite(RELAY_2, HIGH);
    digitalWrite(RELAY_5, HIGH); }
    delay(500);
    lcd.clear(); }

void Beginning (){
  SOC_Value = analogRead(ADC_READ);
  lcd.setCursor(12,0);
  lcd.print(SOC_Value);


lcd.setCursor(0,0);
  lcd.print(Status);

 if (SOC_Value >= 890) bat_percent = 100;
 else if (SOC_Value >= 840)
   bat_percent = map(SOC_Value, 840, 890, 95,
100);
 else if (SOC_Value >= 700)
   bat_percent = map(SOC_Value, 700, 840, 20, 95);
 else if (SOC_Value >= 683)
   bat_percent = map(SOC_Value, 683, 700, 0, 20);
 else bat_percent = 0;
 Serial.print("Battery:");
 Serial.print(bat_percent);
 Serial.println("%");
 Serial.print("SOC:");
 Serial.print(SOC_Value);
 Serial.println("");
 lcd.setCursor(0,1);
 lcd.print("SOC: ");
 lcd.print(bat_percent);
 lcd.print(" %");
}

void switch_motor(){
 toggleSwitch.loop();
 if (toggleSwitch.isPressed()){
  Serial.println("The switch: OFF -> ON");
  digitalWrite(RELAY_3, HIGH);
  digitalWrite(RELAY_4, HIGH);
  delay(10000);
  digitalWrite(RELAY_4, LOW); // Normally Open,
 }
```

```
 if (toggleSwitch.isReleased()){
  Serial.println("The switch: ON -> OFF");
  digitalWrite(RELAY_4, HIGH);
  digitalWrite(RELAY_3, HIGH);
  delay(10000);
  digitalWrite(RELAY_3, LOW); // Normally Open,
 }
 int state = toggleSwitch.getState();
 if (state == HIGH){
  Serial.println(state);
  Serial.println("The switch: OFF/50Hz");
  } // Normally Open,  }
 else if (state == LOW){
  Serial.println(state);
  Serial.println("The switch: ON/60Hz");
}
}

void resetLCD(){
 lcd.home();
 lcd.print(" ");
 lcd.setCursor(0,1);
 lcd.print(" ");
 lcd.home();
 delay(50);
}
```

C. Additional information and formulas

Power Formula

P=I×V (kW)

Where:

P represents power measured in watts (W)

V is the voltage measured in volts (V)

I is the current measured in amperes (A)

Charge Time Formula

Charge (A×h) = I ×t /1000

Where:

Charge is the charge of the battery measured in amperes × hour (A×h)

I is the current measured in amperes

t is the time measured in hours

State of Charge Formula

$$SOC_t = SOC_0 - \frac{Q_i}{Q_0} \times 100\% = SOC_0 - \frac{1}{Q_0}\int \eta I_{(t)} dt \times 100\%$$

Where:

(SOC)t is the remaining power of the battery at time t,

$\boldsymbol{Q0}$ indicates the rated capacity of the battery,

$\boldsymbol{Qi}$ represents the amount of power released by the battery from 0 to t,

$\boldsymbol{I(t)}$ represents the current and takes the direction of battery discharge current as positive,

and $\boldsymbol{\eta}$ is the charging and discharging efficiency.

Basic Power Formula

$P = I^2R$,

Where:

I represents the current

R is the internal resistance of the battery.

Formula, DC-DC Converter

V1=N×V2

I2=N×I1

Where:

V1 is the primary voltage.

V2 is the secondary voltage.

I1 is the current flowing into the primary + terminal.

I2 is the current flowing out of the secondary + terminal.

N is the winding ratio.

Horsepower to Watts Conversion Formula

$$\frac{HP}{N \times Pf \times \frac{\sqrt{3}}{746}} = W$$

Where:

N=efficiency

PF=Power Factor

The block accounts for torque dependent losses:

$$P_{losses} = k\tau_{elec}^2,$$

Where,

$$k = \frac{\omega_\eta(1 - \eta/100)}{\tau_\eta \cdot \eta/100}.$$

The electrical power loss is calculated by,

$$P_{elec} = P_{losses} + \omega\tau_{elec},$$

Joule's law defines the rate at which electrical energy is transformed into heat energy where the heat generated is proportional to the resistance of the wire.

$$I = \frac{P_{elec}}{V},$$

Pelec is the electrical power that the block calculates and uses in the governing equation.

Plosses is the electrical power lost during operation. When you model the effects of heat flow and temperature change, this value represents the rate of heat flow that gets distributed into the thermal mass or out port H.

$\boldsymbol{\omega}$ is the angular velocity of the rotor.

$\boldsymbol{\tau}$elec is the saturated torque demand.

k is the proportionality constant for resistance losses, which has the units (energy*time)-1.

$\boldsymbol{\eta}$ is the efficiency of the motor and driver for a given speed and torque.

$\boldsymbol{\omega_\eta}$ is the angular velocity that corresponds to the overall efficiency. This value is equivalent to the Speed at which efficiency is measured parameter.

$\boldsymbol{\tau_\eta}$ is the torque that corresponds to the overall efficiency.

V is the voltage across the terminals.
I is the current through the terminals.

The efficiency, η, value is equivalent to the motor and driver overall efficiency parameter. The angular velocity that corresponds to the overall efficiency, ω_η, is equivalent to the Speed at which efficiency is measured parameter. The torque that corresponds to the overall efficiency, τ_η, is equivalent to the Torque at which efficiency is measured parameter.

There are assumptions and limitations of the Motor and Block. The first assumption is the torque demand is tracked with the time constant Tc. The second assumption is that the motor torque tracking is not affected by the motor speed fluctuations due to mechanical load.

DC-DC Converters are electronic systems designed to transform a direct current (DC) voltage into a different level of DC voltage, commonly ensuring a consistent and regulated output. An ideal DC-DC voltage converter represents a theoretical model with perfect efficiency and precision in voltage transformation. In this theoretical construct, the converter operates with 100% efficiency, converting an input DC voltage to a desired output DC voltage without any energy losses. It maintains a stable and regulated output voltage without any drop across its components, regardless of load variations or changes in input voltage. This ideal converter exhibits instantaneous response and adapts seamlessly to fluctuations in input or load, ensuring a consistent output voltage, [32].

The battery of the vehicle is a DC voltage source with an internal resistance, voltage sensor, and current sensor. The internal resistance of a DC battery serves several essential purposes within the functioning of the battery system. The internal resistance plays a role in regulating the battery's voltage output. For the simulation, the internal resistance was set to 0.05 Ω. When a load connects to the battery, this internal resistance causes a drop in voltage across the battery terminals, impacting the actual voltage available. This voltage regulation ensures that the battery delivers a consistent and stable voltage. The voltage and current sensors reflect the ideal voltage and currents by converting the voltage and current measured between two points of the circuit and displaying the signals that correspond to the measured values, [31].

Contribution of Individual Authors to the Creation of a Scientific Article (Ghostwriting Policy)

The authors equally contributed to the present research at all stages from the formulation of the problem to the final findings and solution.

Sources of Funding for Research Presented in a Scientific Article or Scientific Article Itself

No funding was received for conducting this study.

Conflict of Interest

The authors have no conflicts of interest to declare.